

Nature of Phosphorus Limitation in the Ultraoligotrophic Eastern Mediterranean

T. F. Thingstad,^{1*} M. D. Krom,² R. F. C. Mantoura,^{3,4}
G. A. F. Flaten,¹ S. Groom,³ B. Herut,⁵ N. Kress,⁵ C. S. Law,^{3,6}
A. Pasternak,⁷ P. Pitta,⁸ S. Psarra,⁸ F. Rassoulzadegan,⁹ T. Tanaka,^{1,9}
A. Tselepidis,⁸ P. Wassmann,⁷ E. M. S. Woodward,³
C. Wexels Riser,⁷ G. Zodiatis,¹⁰ T. Zohary¹¹

Phosphate addition to surface waters of the ultraoligotrophic, phosphorus-starved eastern Mediterranean in a Lagrangian experiment caused unexpected ecosystem responses. The system exhibited a decline in chlorophyll and an increase in bacterial production and copepod egg abundance. Although nitrogen and phosphorus colimitation hindered phytoplankton growth, phosphorus may have been transferred through the microbial food web to copepods via two, not mutually exclusive, pathways: (i) bypass of the phytoplankton compartment by phosphorus uptake in heterotrophic bacteria and (ii) tunnelling, whereby phosphate luxury consumption rapidly shifts the stoichiometric composition of copepod prey. Copepods may thus be coupled to lower trophic levels through interactions not usually considered.

The eastern Mediterranean Sea is a large body of ultraoligotrophic (1) water where both nutrient stoichiometry (2), bioassays (3–6), and P-cycle studies (7) have suggested P limitation of biological production. We performed the Cycling of Phosphorus in the Eastern Mediterranean (CYCLOPS) experiment in the eastern Mediterranean near the center (33.3°N, 32.3°E) of the quasi-stable, warm-core Cyprus Eddy (Fig. 1). The area was studied for 4 days before the release of phosphate on 17 May 2002. Diluted phosphoric acid was added to an ~16-km² patch to a concentration of ~110 nM (8). Vertical spreading was restricted by the seasonal pycnocline at 16 m. The patch, defined by the simultaneous addition of an SF₆ inert tracer, was monitored for 9 days with biological and chemical investigations at stations located in the center of the patch (IN stations). On every other day, the ship moved to a minimum distance of 15 km from the patch center for vertical profiling at an OUT station.

¹Department of Biology, University of Bergen, Bergen, Norway. ²School of Earth and Environmental Sciences and Earth and Biosphere Institute, Leeds University, Leeds, UK. ³Plymouth Marine Laboratory, Plymouth, UK. ⁴Marine Environment Laboratory, International Atomic Energy Agency, Monaco. ⁵Israel Oceanographic and Limnological Research (IOLR), National Institute of Oceanography, Tel Shikmona, Haifa, Israel. ⁶National Institute of Water and Atmospheric Research, Wellington, New Zealand. ⁷Norwegian College of Fishery Science, University of Tromsø, Tromsø, Norway. ⁸Hellenic Centre for Marine Research, Heraklion, Crete, Greece. ⁹Station Zoologique, Villefranche-sur-mer, France. ¹⁰Oceanography Centre, University of Cyprus, Nicosia, Cyprus. ¹¹IOLR, Kinneret Limnological Laboratory, Tiberias, Israel.

*To whom correspondence should be addressed.
E-mail: frede.thingstad@bio.uib.no

Pre-experiment investigations confirmed the ultraoligotrophic status of the surface waters, which had chlorophyll concentrations of $18 \pm 1 \mu\text{g of chl m}^{-3}$ (Fig. 2A) and a daily primary productivity of $29 \mu\text{mol of C m}^{-3} \text{ day}^{-1}$. Pigment analysis of size-fractionated material indicated that most (~65%) of the chlorophyll a (chl-a) was in the picoplankton (<2 μm) fraction with a large (~40% of total chl-a) cyanobacterial component.

After deep mixing in the winter months, dissolved phosphate in the surface waters remained below our detection limits, whereas there is typically a small residual (300 to 500 nM) of nitrate (2, 9). This nitrate was isotopically heavy, which is characteristic of a

phytoplankton bloom that has ceased because of P limitation (10).

By May, both phosphate and nitrate concentrations were below the detection limit (~2 nM) of the nanomolar technique used (8). Using a titrimetric bioassay method based on alkaline phosphatase activity, we estimated the system to contain $\sim 230 \pm 60 \text{ nM residual N}$ (5), which suggests that a large fraction of the residual N had been retained in the system in a form available to at least some components of the biota. Ammonium, determined to 60 to 80 nM N, may have accounted for about one-third of this excess N; the form of the remaining is unknown. The surface waters also contained 65 to 100 μM dissolved organic carbon (DOC), 3 to 11 μM dissolved organic nitrogen (DON), and ~50 nM ultraviolet-oxidizable dissolved organic phosphorus (DOP). All physiological and biogeochemical indicators examined pointed to a P-starved system: The DON/DOP molar ratio was 60:1 to 200:1, the PON/POP ratio was 30:1, and there was alkaline phosphatase activity in surface waters outside the patch (5). Despite the low biomass (7 to 10 nM POP) (Fig. 2B), turnover time for orthophosphate was low for a marine system (2 to 4 hours) (Fig. 3). Combining biomass and turnover time gave us a conservative estimate of the affinity constant for orthophosphate uptake of $\sim 0.08 \text{ liter nM-P}^{-1} \text{ h}^{-1}$ (supporting online text), consistent with what would be expected for orthophosphate uptake limited by molecular diffusion in water (11). Maximum potential for orthophosphate uptake was determined as $1.6 \pm 0.2 \mu\text{mol P m}^{-3} \text{ h}^{-1}$, which is about one order of magnitude above the P demand that can be calculated from a stoichiometric conversion of bacterial and primary carbon production (supporting online text).

From the SF₆ tracer (Fig. 3), we estimated a lateral diffusion coefficient for the patch of

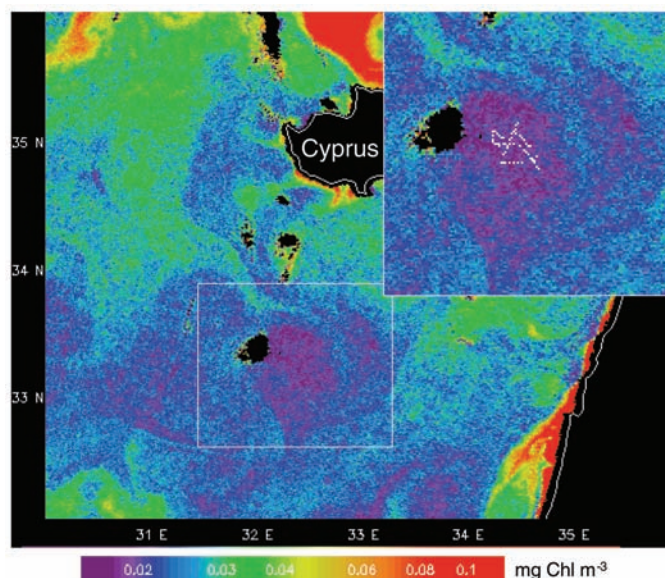


Fig. 1. SeaWiFS satellite chl-a image of the eastern Mediterranean on 25 May 2002, showing the experimental area (inset) in the center of the oligotrophic Cyprus Gyre (the cruise track is in white). The color scale is in mg of chl-a m⁻³. The black patch to the west of the experimental area is a cloud.

$21 \pm 2 \text{ m}^{-2} \text{ s}^{-1}$, corresponding to an initial dilution rate of the P-fertilized patch of ~ 1.0 to 1.2 day^{-1} , decreasing rapidly to $\sim 0.1 \text{ day}^{-1}$ after day 6. This corresponds to a theoretical dilution of the added P to a nominal level of $\sim 15 \text{ nM}$ after ~ 7 to 8 days. Given a

Redfield N:P ratio of 16:1 (molar), the estimated excess N of 230 nM N would correspond to a requirement of $\sim 14 \text{ nM}$ P for its consumption. One would thus expect the system, through N import by physical mixing, to return to its original P-limited state after

~ 1 week. This scenario is confirmed by the measured orthophosphate turnover time, which increased more than 20-fold after P addition. By 1 week after addition, turnover time had returned to < 10 hours (Fig. 3), and orthophosphate concentration had returned to values below our detection limit ($\sim 2 \text{ nM}$).

If all of the assayed 230 nM excess N (5) was assimilated by *Synechococcus* sp., and assuming a N:chl-a ratio of $0.31 \text{ nmol N per ng of chl-a}$ for P-replete *Synechococcus* sp. (12, 13), this would, in the absence of dilution and grazing, correspond to a potential for an ~ 40 -fold increase in chlorophyll (from 18 to $741 \mu\text{g of chl-a m}^{-3}$). Instead, the system responded to the addition of phosphate with a decrease of chl-a in the patch of $\sim 40\%$ (Fig. 2A) [one-way analysis of variance (ANOVA) comparing samples inside the patch with samples taken outside the patch and before the experiment, $P < 0.05$], reaching a minimum of $11 \mu\text{g of chl-a m}^{-3}$ after 5 days. Chlorophyll levels returned to background levels after ~ 1 week. There were also decreasing trends in primary production and in phytoplankton growth rates, while picophytoplankton and smaller nanophytoplankton were reduced in numbers (by 49 and 65%, respectively) within the first 4 days of the experiment. With the precision obtainable in this type of experiment, precise estimates cannot be given for the contributions of growth (μ) and loss rate (γ) to the net change in chlorophyll. When corrected for dilution, a rough estimate suggests a post-addition net loss of $\mu - \gamma \approx -0.6 \text{ day}^{-1}$, equally partitioned between a decrease in μ and an increase in γ (supporting online text).

In an on-deck microcosm experiment, ammonium was added or not to water collected inside or outside the P-fertilized patch. Ammonium addition induced a phytoplankton bloom in water collected inside the patch but not in water collected outside the patch (fig. S1) (supporting online text). The in situ finding that adding P alone leads to increased particulate P and bacterial production but not phytoplankton production was replicated in the microcosms. This demonstrated the N-limited state of phytoplankton after P addition and indicates that the assayed excess N was not available to phytoplankton over this time scale. The natural system, despite clear indications of P starvation and excess N, could thus be described as colimited by N and P for phytoplankton.

N_2 fixation has been proposed as an important mechanism driving the Mediterranean toward P limitation (14). If N_2 fixation played a role in our experiment, however, either it was insufficient to produce a positive net response in phytoplankton or it occurred in heterotrophs. In contrast to the negative trend in phytoplankton response, particulate P (Fig. 2B) had almost doubled already at the first

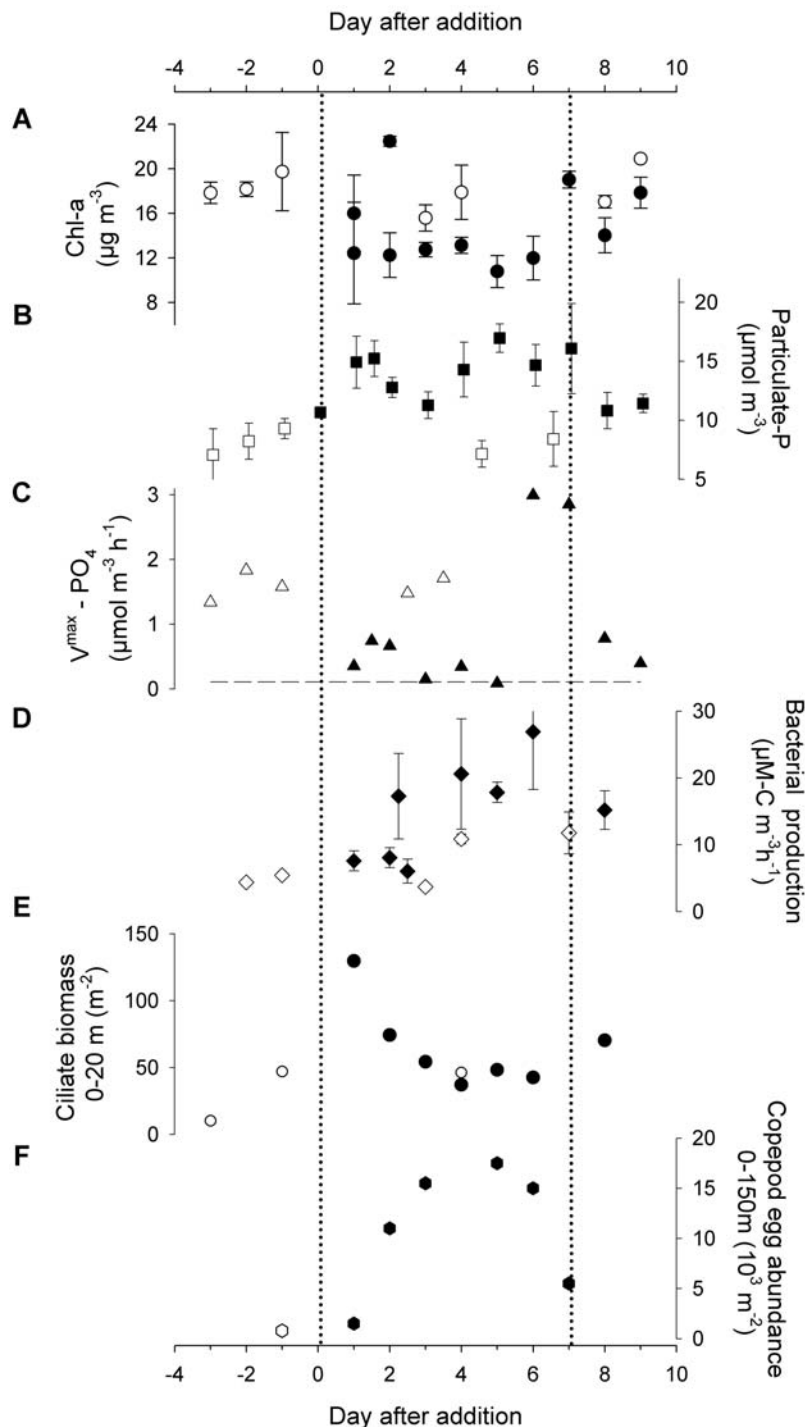


Fig. 2. Biological responses in the top layer: (A) High-pressure liquid chromatography-measured chl-a (circles), (B) particulate P (squares), (C) maximum uptake potential for orthophosphate (triangles, V_{max}), and (D) bacterial production (diamonds), all averaged over depths $< 20 \text{ m}$. Error bars show the SE of samples (generally four) taken within the 0- to 16-m layer and thus contain both experimental error and natural variations within the top layer. (E) Ciliate biomass integrated over 0 to 20 m (circles) and (F) abundance of copepod eggs integrated over 0 to 150 m (hexagons). Open symbols indicate samples taken before or outside the patch; solid symbols, samples taken inside the patch.

sampling after addition, concurrent with a drop in the maximum potential for orthophosphate uptake (Fig. 2C). This is the pattern that would be expected for phytoplankton (15) and heterotrophic bacteria (16) rapidly replenishing their internal cell quota for P and reducing their maximum uptake capacity to the level required for growth.

There was an increase in bacterial production (ANOVA, comparing measurements before and inside the patch, $P < 0.001$) (Fig. 2D). Bacterial abundance ranged from 0.6 to 1.4×10^{11} cells m^{-3} , with no clear trend between samples taken inside and outside the patch. We suggest that the nitrogen and organic C required to support this increased bacterial production may be from the DON and DOC pools, respectively.

Copepod egg abundance in the water column increased by more than one order of magnitude, a response visible after 2 days and

peaking after 5 days (Fig. 2F). There may also have been a positive response in ciliate abundance peaking on the first day after addition (Fig. 2E) (day 1 was significantly different from days -3 and -1, and from days 5, 6, and 8, $P < 0.01$), then disappearing rapidly.

We propose two, not mutually exclusive, trophic pathways for transfer of the added P to copepods. One is a “trophic bypass” whereby added P bypasses the phytoplankton compartment through a predatory food chain from heterotrophic bacteria (Fig. 4), producing a concomitant increase in predation loss (γ) of small-celled phytoplankton. Support for such a mechanism can be found in our stimulated bacterial production (Fig. 2D). Another possible route for P transfer is by “trophic tunnelling,” in which phosphate “disappears” through rapid luxury consumption into phytoplankton and bacteria, thus changing the stoichiometry but not the abundance of prey organisms. If there

are predator processes such as ciliate DNA synthesis or copepod egg production that are P-limited, the added P would “reappear” as responses at the predator level much more rapidly than could be expected from models that transport P through nutrient-prey-predator successions in a food chain of organisms with fixed biomass stoichiometry.

The bypass mechanism would be in agreement with previous observations indicating P limitation of heterotrophic bacteria in the eastern Mediterranean (4), implying that there are components in the large DOC and DON pools accessible to bacteria. The relative importance of this bypass route would be enhanced if heterotrophic bacteria have better access than phytoplankton to the system’s pool of excess N. A likely candidate would be dissolved combined amino acids, usually believed to be primarily accessible by heterotrophic bacteria. This would imply that there are mechanisms in the system converting any nitrate remaining after the winter phytoplankton bloom to DON in the summer, thus converting an apparently conventionally defined P-limited system to one where phytoplankton are colimited by P and N. Extreme situations with pure N limitation of autotrophs while bacteria are P-limited have recently been described in coastal wetlands (17).

However, the sequence where ciliate (Fig. 2E) and copepod (Fig. 2F) responses occur before any detectable increase in bacterial production (Fig. 2D) is difficult to reconcile with bypass as the only trophic transport of P. Because P acquired by luxury consumption cannot be translated into biomass production in the absence of available N, lack of access to the excess N pool would leave the phytoplankton with a high P cell quota. Estimating osmotroph C biomass to ~50% of total particulate C, the approximate doubling in total particulate P may have represented an ~4 times increase in the osmotroph cell quotas. The amount of P transported per prey into the predator food chain must have increased accordingly. It is thus reasonable to adapt the limnologist’s hypothesis of P-starved mesozooplankton (18). A change in food quality (P content), rather than in food quantity (abundance), is thus suggested as the main signal initiating egg production in copepods and possibly also cell division in ciliates, shortly after the orthophosphate addition. If, in addition to the traditional luxury consumption, there was a surface adsorption of added phosphate to phytoplankton (19), this would add to the proposed tunnelling transport.

Implicit in this scenario is that heterotrophs use the time between nutrient pulses to store carbon (energy) and nitrogen, bacteria possibly in extracellular forms (such as DOC and DON) and zooplankton probably as somatic storage material. Both groups would then be able to respond once P becomes available, as orthophosphate or as P-enriched prey, respectively.

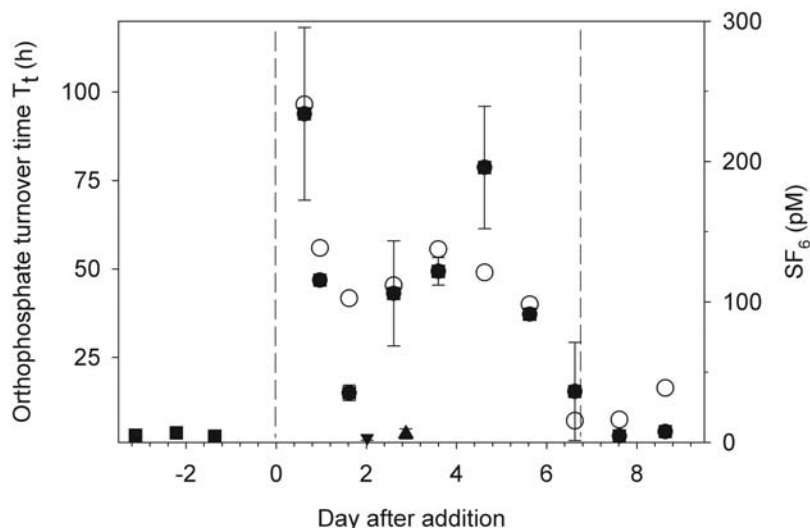


Fig. 3. SF₆ concentrations (○) and orthophosphate turnover time (T_t) before (■), inside (●), outside (▼), and below (▲) the patch. Vertical dotted lines indicate the experimental release and the estimated time of return of the system from N to P limitation. Error bars indicate SE of four samples taken inside the 0- to 16-m layer.

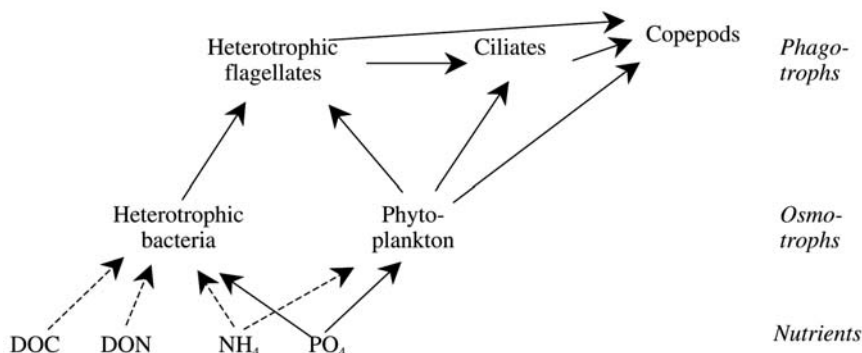


Fig. 4. Idealized model of the P flow (solid arrows) through the lower part of the pelagic food web. We suggest that the added P can be transported to the level of phagotroph predators either through bypass, in which heterotrophic bacteria can produce biomass because of access to parts of the DON pool, or by tunnelling, in which luxury consumption increases the cell quota of P in osmotrophs, thus changing the quality but not the quantity of prey for P-limited predators. Other potentially limiting nutrients are indicated by broken arrows. The remineralization process is omitted for clarity.

With a summer situation characterized by P-limited bacteria and grazers, whereas phytoplankton are closer to an N and P colimitation, nature of the P limitation in the eastern Mediterranean becomes both seasonally variable and organism-dependent. Although our interpretation requires a much more elaborate conceptual model of the pelagic food web than is needed to explain the more conspicuous response of a phytoplankton bloom observed when iron has been added in high nutrient, low chlorophyll (HNLC) areas, the interpretation introduces no fundamentally new biological mechanisms.

Within our proposed interpretation, the counterintuitive combination of a negative chlorophyll response with a positive zooplankton response is a function of the oligotrophy, the P limitation, and the form in which excess N is stored and is thus linked to particular biogeochemical features of the post-bloom eastern Mediterranean ecosystem. Flexible stoichiometry, alternative microbial food chains, and differential access to pools of the next limiting element may be sophistications that can be disregarded in some biogeochemical models. In the eastern Mediterranean with its pulsed atmospheric nutrient inputs from Saharan dust storms, such trophic “sophistications” may however be the key to central aspects of ecosystem functioning.

Copepods are believed to have a central role not only in bridging production in the microbial

part of the food web to commercially interesting fish resources but also as producers of vertical export of C, N, and P to the ocean’s interior. With a low nutrient, low chlorophyll state being the dominant mode in the world’s surface oceans, an increasing awareness of P-limited oceanic regions (20–24), and an increasing trend toward a high N:P in atmospheric inputs (25), these results are likely to be relevant not only to the eastern Mediterranean but also to large areas of today’s oceans and their response to global change.

References and Notes

1. A. C. Redfield, B. H. Ketchum, F. A. Richards, in *The Sea*, M. N. Hill, Ed. (Wiley, New York, 1963), vol. 2, pp. 26–77.
2. M. D. Krom, N. Kress, S. Brenner, L. I. Gordon, *Limnol. Oceanogr.* **36**, 424 (1991).
3. D. J. Bonin, M. C. Bonin, T. Berman, *Aquat. Sci.* **51**, 129 (1989).
4. T. Zohary, R. D. Robarts, *Limnol. Oceanogr.* **43**, 387 (1998).
5. T. F. Thingstad, R. F. C. Mantoura, *Limnol. Oceanogr. Methods* **3**, 94 (2005).
6. F. Van Wambeke, U. Christaki, A. Giannakourou, T. Moutin, K. Souvemerzoglou, *Microb. Ecol.* **43**, 119 (2002).
7. T. Moutin *et al.*, *Limnol. Oceanogr.* **47**, 1562 (2002).
8. Materials and methods are available as supporting material on Science Online.
9. N. Kress, B. Herut, *Deep-Sea Res. I* **48**, 2347 (2001).
10. U. Struck, K.-C. Ernie, M. Voss, M. D. Krom, G. H. Rau, *Geochim. Cosmochim. Acta* **65**, 3249 (2001).
11. T. F. Thingstad, F. Rassoulzadegan, *Prog. Oceanogr.* **44**, 271 (1999).

12. S. Bertilsson, O. Berglund, D. M. Karl, S. W. Chisholm, *Limnol. Oceanogr.* **48**, 1721 (2003).
13. S. W. Jeffrey, H. S. MacTavish, W. C. Dunlap, M. Vesik, K. Groenewoud, *Mar. Ecol. Prog. Ser.* **189**, 35 (1999).
14. J. P. Béthoux, P. Morin, D. Ruiz-Pino, *Deep-Sea Res. II* **49**, 2007 (2002).
15. H. Ducobu, J. Huisman, R. R. Jonker, L. R. Mur, *J. Phycol.* **34**, 467 (1998).
16. O. Vadstein, *Aquat. Microb. Ecol.* **14**, 119 (1997).
17. P. V. Sundareswar, J. T. Morris, E. K. Koepfler, B. Fornwalt, *Science* **299**, 563 (2003).
18. T. Andersen, J. J. Elser, D. O. Hessen, *Ecol. Lett.* **7**, 884 (2004).
19. S. A. Sanudo-Wilhelmy *et al.*, *Nature* **432**, 897 (2004).
20. J. Ammerman, R. Hood, D. Case, J. Cotner, *Eos* **84**, 165 (2003).
21. S. A. Sanudo-Wilhelmy *et al.*, *Nature* **411**, 66 (2001).
22. J. F. Wu, W. Sunda, E. A. Boyle, D. M. Karl, *Science* **289**, 759 (2000).
23. D. M. Karl *et al.*, *Deep-Sea Res. II* **48**, 1529 (2001).
24. M. M. Mills, C. Ridame, M. Davey, J. La Roche, R. J. Geider, *Nature* **429**, 292 (2004).
25. T. Jickells, in *Challenges of a Changing Earth*, W. Steffen, J. Jäger, D. J. Carson, C. Bradshaw, Eds. (Springer-Verlag, New York, 2002), pp. 93–96.
26. We wish to thank the crew of research vessel *Aegaeo* for companionship and assistance, and P. Carbo for her invaluable help in administering the whole program. This project was funded by the European Union through project no. EVK3-CT-1999-00009, “CYCLOPS”.

Supporting Online Material

www.sciencemag.org/cgi/content/full/309/5737/1068/DC1

Materials and Methods

SOM Text

Fig. S1

References and Notes

23 March 2005; accepted 12 July 2005

10.1126/science.1112632

Direct Control of Germline Stem Cell Division and Cyst Growth by Neural Insulin in *Drosophila*

Leesa LaFever and Daniela Drummond-Barbosa*

Stem cells reside in specialized niches that provide signals required for their maintenance and division. Tissue-extrinsic signals can also modify stem cell activity, although this is poorly understood. Here, we report that neural-derived *Drosophila* insulin-like peptides (DILPs) directly regulate germline stem cell division rate, demonstrating that signals mediating the ovarian response to nutritional input can modify stem cell activity in a niche-independent manner. We also reveal a crucial direct role of DILPs in controlling germline cyst growth and vitellogenesis.

Germline and somatic stem cells support oogenesis throughout adult life in *Drosophila* (1) (fig. S1). Germline stem cells (GSCs) reside within a specialized niche where they are exposed to a unique combination of signals required for stem cell function (2, 3). However, GSCs are also controlled by tissue-extrinsic

signals, such as *Drosophila* insulin-like peptides (DILPs), which mediate the ovarian response to nutrition (4). On a protein-rich diet, germline and somatic stem cells have high division rates, and their progeny exhibit high division and development rates. On a protein-poor diet or under reduced insulin signaling, rates of division and development are reduced, and progression through vitellogenesis is blocked (4). It remains unclear, however, how DILPs control the response of GSCs in coordination with their differentiating progeny and with follicle cells.

In adult females, DILPs are produced in two clusters of medial neurosecretory cells in the brain (5), and stage 10 follicle cells express *dilp5* mRNA (6). Ablation of brain DILP-producing cells results in reduced egg production rates and a partial block in vitellogenesis (6). To examine the role of the brain DILP-producing cells in previtellogenic stages, we ablated them and measured follicle cell proliferation rates (7) (fig. S2). Females missing brain DILP-producing cells (ablated) have a severely impaired ability to up-regulate follicle cell proliferation in response to a protein-rich diet (Fig. 1). The rate of germline development is reduced in coordination with follicle cell divisions because no abnormalities are observed in previtellogenic egg chambers (8). Ablation of DILP-producing cells reduces the size of eclosed adults and delays development (9). Ablated females in which these developmental defects are rescued by an *hs-dilp2* transgene expressed during larval stages show a reduced follicle cell proliferation rate, comparable to that of nonrescued, ablated females (Table 1). Thus, the impaired response to a protein-rich diet is not a secondary consequence of the developmental defects. Moreover, the 2.3-fold delay caused by ablation of brain DILP-producing cells (7) is very similar to that caused by blocking reception of DILP signals by the germ line (below). This indicates that

Department of Cell and Developmental Biology, Vanderbilt University Medical Center, 4120B Medical Research Building III, 465 21st Avenue South, Nashville, TN 37232–8240, USA.

*To whom correspondence should be addressed. E-mail: daniela.drummond-barbosa@vanderbilt.edu